Fractionation and Characterization of Linear Low-Density Polyethylene at a Lower Critical Solution Temperature (LCST)

ALLA BARBALATA, TAKOUHI BOHOSSIAN, and GENEVIÈVE DELMAS*

Chemistry Department, Université du Québec à Montréal C.P. 8888, succursale "A," Montréal, Québec, Canada H3C 3P8

SYNOPSIS

The composition and molecular weight distribution of linear low-density polyethylenes (LLDPE) have been determined by fractionation and characterization at a lower critical solution temperature (LCST). The fractionation in 2,4-dimethyl pentane takes advantage of the fact that the LCST is sensitive to the side-group content as indicated by the 70 K difference between the LCSTs of PE and polypropylene at the same molecular weight (MW). Temperature-rising elution fractionation (TREF) and LCST fractions are compared by IR and SEC and also by a new method based on turbidity at an LCST. It is found that the LCST fractionation is sensitive to MW and TREF largely depends on a comonomer content. Calibration of the LCST method for MW distribution and effect of the nature of the comonomer on the LCST are discussed. The LCST technique associated with IR analysis is found to be quite effective for characterizing LLDPE.

INTRODUCTION

A wide range of desirable properties for polyethylene (PE) resins can now be obtained by polymerization of ethylene and another alcene such as butene, hexene, or octene. The characteristics of the resulting product, linear low density polyethylene (LLDPE), such as density, viscosity of the melt, modulus, and tensile and tear strength, can be improved and controlled by varying the percentage of comonomer, the reactor conditions, or the catalyst. LLDPE can be synthesized so that the monomer content does not have an effect on chain length.[1-3] However, extensive work[4-12] made on industrial LLDPE shows that the large-scale method of preparation leads to the production of heterogeneous polymers. The multipeak DSC traces found for LLDPE reveal a range of crystallinity in the sample. The SEC technique, which is sensitive to molecular size in solution but insensitive to chemical constitution, does not detect the

heterogeneity of the chains. The temperature-rising elution fractionation technique (TREF) has been successful[6] in achieving a continuous separation by crystallinity or comonomer content of industrial LLDPE. This is possible because the dissolution temperature of a sample in an aromatic solvent, for instance, drops from 100°C to room temperature when the number of methyl group per 1000 carbon atoms increases from 5 to 20.

Analyses by different techniques[7-9] of industrial and laboratory LLDPE samples led to the conclusion that their heterogeneity is extensive and depends on the process of synthesis. For many but not all the samples prepared in solution, the comonomer content increases when the chain length diminishes.

The aim of this paper is to present data on fractions prepared at a lower critical solution temperature (LCST). The characteristics of the LCST fractions (composition and MW) will be compared to those of TREF fractions. Further analysis of polydispersity will be made by a new method of polymer characterization based on the quantitative measurement of turbidity at an LCST described previously.[13-15]

The Lower Critical Solution Temperature

The discovery almost 30 years ago of the occurrence of a phase separation at high temperature in nonpolar polymeric solutions[16] was interpreted in terms of a new theory of polymer thermodynamics that was more appropriate than the lattice theory to describe the polymer solutions.[17-22] Since theoretical and experimental work has been published on this topic,[15,20] only a brief resume of the phase separation at an LCST relevant to the present work will be given below.

A diminution of the solvent quality when the temperature is increased is due to a inescapable difference of expansion between the solvent above its boiling point and the dense polymer. Using an equation of state suited to describe liquids of different molar size (from a monomer to a polymer), Prigogine, Patterson, Flory, et al. could predict the occurrence of LCST in nonpolar systems and relate its values to parameters of the pure components.[17-21]

Case of Polyethylene and Polypropylene

Analysis of the LCST of several polyolefins in nonpolar solvents[23] has shown that polyethylene had LCST values that were lower than those of the other polyolefins under the comparable equation of state parameters. The difference between the LCST of PE and polypropylene (PP), for instance, which can reach 70 K in a volatile solvent, for the same molecular weight (MW), has been explained in terms of correlations of molecular orientations (CMO) in the concentrated phase of PE. In PE solutions, the free energy of the system can be minimized by forming a concentrated phase where CMO are more probable than in the dilute solution. By preventing some of the CMO to form, the side groups in LLDPE raise the LCST.

EXPERIMENTAL

Solvent: The branched heptane, 2,4 dimethylpentane (99%, Aldrich Co., Milwaukee, WI) was used without purification.

Polymers: The polymers analyzed are LLDPE from the Du Pont Company (Kingston, Ontario). Samples with different comonomer content and melt index have been analyzed. In this paper, the results are reported only on two samples, one with the butylene, E(B), and the other with octene, E(O), as comonomers.

Measurements

SEC and TREF of the samples were done at the DuPont Research Center of Kingston (Ontario) following standard procedures. The methyl content of the samples was measured either on a grating or an FTIR instrument (Digilab). The methyl content of the original polymers and of their LCST and TREF fractions are listed in Table I along with their respective values of M_w and M_w/M_n obtained by SEC.

Fractionation

The TREF fractions were obtained by elution with toluene at different temperatures (cf. Table I) from the polymer that had crystallized slowly on a column.

The LCST fractions were prepared in the following way: A polymer solution (volume fraction 0.03 $< \phi_2 < 0.05$) was prepared at 110°C by rotating gently the sealed tube containing solvent and polymer during 4–8 h. Nitrogen gas was passed through the mixture during 1 h before dissolution to prevent degradation. Then, the temperature was raised very slowly to T_1, which was higher than T_0, the cloud-point temperature. The difference between T_1 and T_0 determines the amount of polymer separated in the first fraction. The turbidity disappears when a sedimentation of the concentrated phase occurs. The concentrated phase richer in high molecular weights than the dilute phase is separated. The process is renewed on the dilute phase whose temperature is raised to $T_2 > T_1$ (cf. Table I).

Characterization by Thermograms

The analysis of a sample can be achieved without the physical separation of the phases as described below. The method developed in the previous works[13-15] is reported here succintly. A sealed tube (inner diameter 5 mm, outer diameter 9 mm, length 7–8 cm) containing 0.6 cm^3 of the solution in 2,4-dimethylpentane is placed in a small oven whose temperature is increased by steps separated by 40–90 min. A beam of light is recorded on a photocell after passing through the upper part of the solution. An increase of temperature does not change the transmitted light when it is effected below T_0. Above this temperature, each step of temperature increment leads to the turbidity due the scattering of light by the heterogeneous system constituted by the droplets of the concentrated phase in the dilute phase. The newly formed concentrated phase ultimately falls to the bottom of the tube, joining those formed previously and leaving the upper dilute so-

Table I Characteristics of PEB and PEO: Original and Fractions

Sample	Temperature of Fractionation (°C)	% of Total	IR Analysis $CH_3/1000$	SEC Analysis		Cloud-Point Curves (T_{min} °C)	
				$10^{-3}M_w$	M_w/M_n	2.4-Dimenthyl Pentane[a]	Pentane + Hexane (1/1)
Original E(B)[b]		100	13.2	40.2	2.8	134	108
Fractions							
LCST1	150	6.3	10-	117.0	4.8	139	107.2
LCST2	150-156	12.5	11.6	67.0	2.4	143	112.5
LCST3	156-166	9.3	13.7	42.3	2.2	150	120
LCST4	166-173	15.0	15.5	35.0	2.2	156	126
LCST5	173-180	8.2	17.2	26.9	2.1	162.5	131.5
LCST6	180-190	7.8	17.8	21.7	2.1	170	134.5
LCST7	190	32.2	19.4	14.9	—	175	138
Original E(B)[b]		100	17.1	41.2	2.9	134	—
Fractions							
TREF5	90.7-126.4	18.0	5	64.1	2.1	134	—
TREF4	80.7-90.7	31.1	13	49.3	2.1	145	—
TREF3	70.4-80.7	26.5	18.3	35.8	2.0	155	—
TREF2	60.3-70.4	11.9	26.1	26.3	1.8	163	—
TREF1	RT-60.3	12.5	30.7	14.0	1.9	175	—
Original E(O)		100	13.3	142	5.4		
Fractions							
TREF5	93.7-126.1	29.7	2.1	218	3.7		
TREF4	85.6-93.7	21.9	8.8	154	3.4		
TREF3	70.4-85.6	33.1	16.1	107	3.2		
TREF2	59.7-70.4	11.1	22	48.7	2.4		
TREF1	RT-70.4	0	—	—			

[a] T_{min} is lower than T_0 in the case of E(B) first because it is a value determined by the minimum of $T(\phi_2)$ curve and also because T_0 is obtained by temperature increments and T_{min} by a temperature ramp.

[b] The two E(B) samples used for TREF and LCST fractionation do not come from the same lot.

lution clear and free of the higher MW. The thermogram of a solution is the set of peaks of attenuation of light, h_i, separated by plateaux of high light transmittance developed in time when the temperature is raised by increments between T_i and $T_i + \Delta T_i$ ($1 < \Delta T_i < 5$ K). The end of the thermogram is marked by the temperature, T_f, at which a temperature increment does not lead anymore to a measurable amount of turbidity in the solution. The assumption on which a quantitative measurement of the MWD rests is of a relationship between the maximum of the peak of turbidity h_i produced by a temperature increase ΔT_i and the amount of polymer (m_i) phase-separating during this temperature interval in the volume of solution under scrutiny.

Quantitative Evaluation of Molecular Weight and Polydispersity

The set of h_i (T_i) of the thermogram has to be converted in quantity of polymer, m_i, and molecular weight, M_i, in order to calculate the average MW and the MW distribution. With the restrictions described in PE[13] and polyisoprene papers,[15] the simple relationship is as follows:

$$T_i = T_\infty + BM_i^{-1/2} \tag{1}$$

where B is a constant and T_∞, the cloud-point temperature for infinite MW, is satisfactory. When the LCST is near the pure solvent critical temperature T_0, an equation of state relationship is preferable to correlate T and M. In the present systems, T/T_c varies among the fractions from 0.78 (beginning of thermogram) to 0.95 (end of thermogram). An equation of state applied to the solution relates the well-known critical value of the interaction parameter, X, to the reduced volume of the solvent, v, and, hence, to the solvent temperature:

$$X \text{ (critical)} = (1 + r^{-1/2})^2$$
$$= c_1\nu^2 f(\tilde{v}) + c_1\tau^2 f'(\tilde{v}) \tag{2}$$

$f(\tilde{v})$ and $f'(\tilde{v})$ are simple functions of $\tilde{v}$; $c_1\nu^2$ corresponds to the chemical difference between solvent and polymer; and $c_1\tau^2$ is the difference in free volume that can be calculated from expansion coefficients of solvent and polymer. In a volatile solvent, the second term in eq. (2) is large and brings down the LCST. In nonpolar systems, $c_1\nu^2$ can be taken as nil. By solving eq. (2), the reduced volume of the solvent, $\tilde{v}$, can be obtained as a function of r or M (r being the ratio of polymer to solvent molar masses). The actual temperature of phase separation is calculated by the two following relations: $T = \tilde{T} \cdot T^*$ and $T = \tilde{v}^{-1}(1 - \tilde{v}^{-1/3})$. T^* is obtainable from the properties of the pure solvent.

The quantity m_i relates to h_i, the normalized turbidity, by

$$m_i = kh_i^n \tag{3}$$

where k is a constant. The simple value $n = 1$ in eq. (3) has been used previously,[13] but a calculation of scattered light using the model of a two-phase system made recently[24] leads to the value of $n = 1.5$. With a given $T = f(M)$ curve, the value of $n = 1.5$ gives a lower polydispersity since the highest peaks are counted more than the smallest ones. To confirm the theoretical prediction, a series of monodisperse and polydisperse samples of PE, iPP and aPP have been analyzed by the LCST technique and their polydispersity compared to the SEC values. It is found that the value $n = 1.5$ leads to better results for polydispersity and that the difference, which is small for monodisperse systems (about 2%), increases for broad MWD. The results are calculated in Table II with $n = 1$, but the values of M_w and M_w/M_n calculated with $n = 1.5$ are not too different for the range of polydispersity of the present samples. As an example, the polydispersity of E(O) TREF3 is found to be 3.3 ($n = 1$) and 2.7 ($n = 1.5$).

Characterization of Heterogeneous Samples Such as LLDPE

To take account of the change in chemical composition with MW, eq. (1) must be replaced by

$$T_i = T(m) + B(m)M^{-1/2} \tag{4}$$

The constants could be obtained from characterized homogeneous fractions with different m. Since these

samples are not commercially available, $T(m)$ and $B(m)$ are estimated from fractions. $T(m)$ is expected to increase, and $B(m)$, to decrease when M_w diminishes. If the equation of state is used, the parameter $c_1\tau^2$ (and eventually $c_1\nu^2$ if it is different from 0) is written as a function of $M[c_1\tau^2 = c_1\tau_0^2(1 + UM^{-1/2})]$ to take into account the heterogeneity of the samples or of the fractions (U being a constant).

Calculation of Averages

The averages MW are calculated from the experimental points $h_i(T_i)$ with

$$Mn = (\sum h_i^* / M_i)^{-1} \quad \text{and} \quad M_w = \sum h_i^* M_i \tag{5}$$

with $h_i^* = h_i / \sum_{i=1}^{i=f} h_i$. If too few points have been taken on the thermogram, especially at low temperature (which is not the case of the data shown on Fig. 4), the averages must be obtained from the smoothed $h_i(T_i)$ cumulative curve. By derivation of the cumulative curve, the MWD is calculated. Cumulative curves can be drawn with other coordinates than those of Figure 4 in order to have direct information on the MWD. An example of such cumulative curve is given in Figure 7 with h_i on a probability paper as ordinate and $\ln M$ as abscissa. If the distribution of MW is ln-normal, the points lie on a straight line and the distribution depends only on two parameters, namely, on M_0, the abscissa of the point whose ordinate is 0.5 and on the slope of the line. The MW distribution goes through a maximum for $M = M_0$ and is symmetrical in relation to a vertical axis going through M_0. The values of M_w and M_n are obtained through the abscissa of the points whose ordinates are, respectively, 0.16 ($\ln M_1$) and 0.84 ($\ln M_2$).[25]

$$M_w = M_0 e^{\sigma^2/2} \quad \sigma = \ln M_1 - \ln M_0$$

$$M_n = M_0 e^{-\sigma^2/2} \quad \sigma = \ln M_2 - \ln M_0 \tag{6}$$

If the experimental points do not follow a straight line, particularly at the high or low M_w range, M_w and M_n cannot be obtained as explained above. The averages are obtained as given in eq. (5) but using small $\ln M$ intervals (0.1).

Table II Characteristics of LLDPE in 2,4-Dimethylpentane by LCST

| | SEC Analysis | | Thermograms (°C) | | | | | LCST Analysis — Calculations | | | | | | |
| | $10^{-3}M_w$ | M_w/M_n | T_0 | $T_{1/2}$ | $T_{1/2} - T_0$ | T_f | $t_\infty =$ | With Eqs. (3)[a] and (4) | | | With Eqs. (2) and (3)[a] | | | |
								$B =$	$10^{-3}M_w$	M_w/M_n	$T*^c$	U^b	$10^{-3}M_w$	M_w/M_n
Original E(B)	40.2	2.8	142	170.5	28.5	227	140	4300	40.6	3.8	5420	−0.1	41.9	2.9
Fractions														
TREF5	64.1	2.1	146	152	6	203	131	4300	65.5	1.9	5390	−0.85	65.4	2.3
TREF3	35.8	2.0	162	168	6	195	141	4300	34.5	1.2	5690	−1.6	35.6	2.1
TREF2	26.3	1.8	171	176.5	5.5	195		4300						
TREF1	14.0	1.9	180	191	11	220	155	4300	14.2	1.2	5920	−1.5	12.8	2.0
LCST2	67.0	2.4	143	149	6	203	134	4300	70.5	2.0	5400	−0.7	12.8	2.2
LCST4	35.0	2.2	156	160	4	195	137	4300	33.8	1.3	5625	−1.5	37.9	2.2
Original E(O)	142	5.4	134	157.5	23.5	202	132	4300	110	7.0	5362	−0.05	137.4	5.5
Fractions														
TREF5	218	3.7	134	144	10	172	130	4300	215	5.0	5320	0	232	3.7
TREF4	154	3.4	143	156	14	188	138.5	4300	125	3.7				
TREF3	107	3.2	158	170	12	227	152.5	4300	102	4.2	5610	−0.3	105.4	3.3
TREF2	48.7	2.4	166	185	17	228	260.5	4300	52.9	2.4	5690	−0.4	47.3	2.4

[a] With $n = 1$.
[b] $c_1 \tau^2 = c_1 \tau_0^2 (1 + UM^{-1/2})$, $c_1 \tau_0^2 = 0.194$.
[c] $T = T* [\bar{v}^{-1}(1 - \bar{v}^{-1/3})]$.

RESULTS AND DISCUSSION

Fractionation

SEC and IR Analysis

Table I gives the characteristics of the unfractionated E(B) and E(O) samples and of their fractions, namely, the TREF fractions for E(B) and E(O) and the LCST fractions for E(B). The successive columns give, starting from the first, for each fraction, the temperature of the fractionation, the percentage of the total sample in that fraction, its methyl content, its SEC analysis, and the minimum of the cloud-point curves in 2,4-dimethylpentane and in a mixture of n-C5 and n-C6.

The heterogeneity of the sample is illustrated by the third column of Table I and by Figure 1, which is a plot of m vs. $M_w^{-1/2}$. From the values of M_w and m of the high MW fractions of LCST and TREF, for instance, LCST1: 117×10^3, 10, TREF5: 64×10^3, 5), one can conclude that the TREF method (curves a and b) is more selective toward the methyl content while the LCST method (curve c) separates preferentially the higher MW in the sample. This is an expected result since the TREF method using a solid–solution equilibrium is very sensitive to methyl content through its effect on crystallinity.
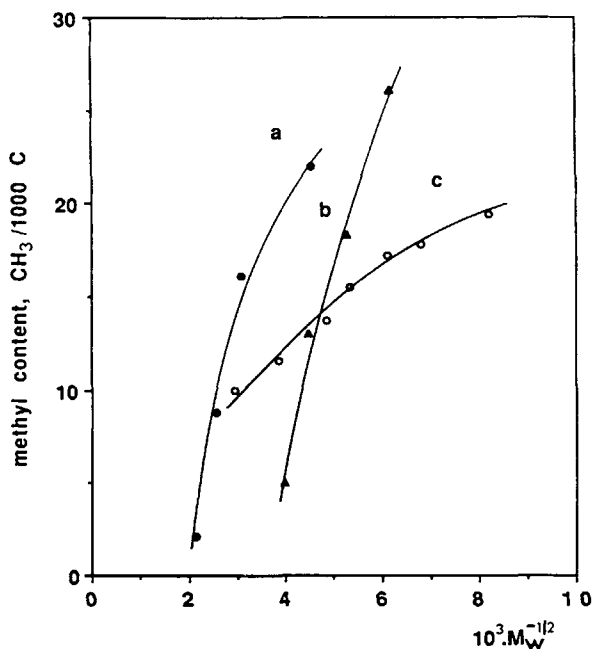
Figure 1 Comparison of the TREF and LCST fractionations: plot of m against $M_w^{-1/2}$. Curves a and b for the TREF fractions of E(O) and E(B) and curve c for the LCST fractions of E(B). The data for curve c are given in Table I.

Fractionation at the LCST using a liquid–liquid equilibrium depends on the chemical potential of the solvent itself, related to molecular weight through the combinatorial entropy and to equation of state parameters through the X parameter. The polydispersities of the TREF and LCST fractions are comparable except for that of LCST1, which is higher, probably because it is a higher MW fraction. The quantity of polymer in the original sample with an MW higher than 10^5 is found on the SEC curve (not given here) to be 6.9%, comparable to the amount of LCST1 whose average M_w is 117,000. It is likely that the last LCST fraction involves partially degraded polymer that was produced by the succession of the seven high-temperature fractionations.

Cloud-Point Curves

The temperature of first turbidity, T_0, has been measured for E(B) and its LCST fractions in a mixture 1/1 by volume of n-C5 + n-C6 and for its TREF fractions in 2,4-dimethylpentane. The mixture of n-C5 and n-C6 was used to test its suitability as a good substitute for the expensive branched heptane. The sample is well soluble in the mixture and phase separation occurs on a similar range of temperature. Figure 2(a) gives the cloud-point curve in n-C5 + n-C6, and Figure 2(b), the minimum of the cloud-point curve, T_{min} vs. m. The linearity between T_{min} and m indicates a relationship between the length of a chain and its methyl content, in agreement with literature results.

The TREF and LCST fractions are compared in Figure 3. The sharp rise in T_{min} vs. $M_w^{-1/2}$ for the TREF fractions (curves b and c) is due to their fast increase in methyl content. The raise in the LCST is smoother for the LCST fractions (curve a).

CHARACTERIZATION BY THERMOGRAMS

Thermograms of the unfractionated E(B) and E(O) samples and of the TREF and LCST fractions have been obtained and their characteristic temperatures in 2,4-dimethylpentane are listed in Table II. For some of the LCST fractions, the cloud-point curves and SEC data were not obtained due to the lack of samples.

Cumulative Curves

The thermograms consist of 20–25 peaks between 130 and 223°C. On the original nonfractionated E(B) sample, a singularity occurs; two small peaks come out at low temperatures, 142 and 144°C, fol-
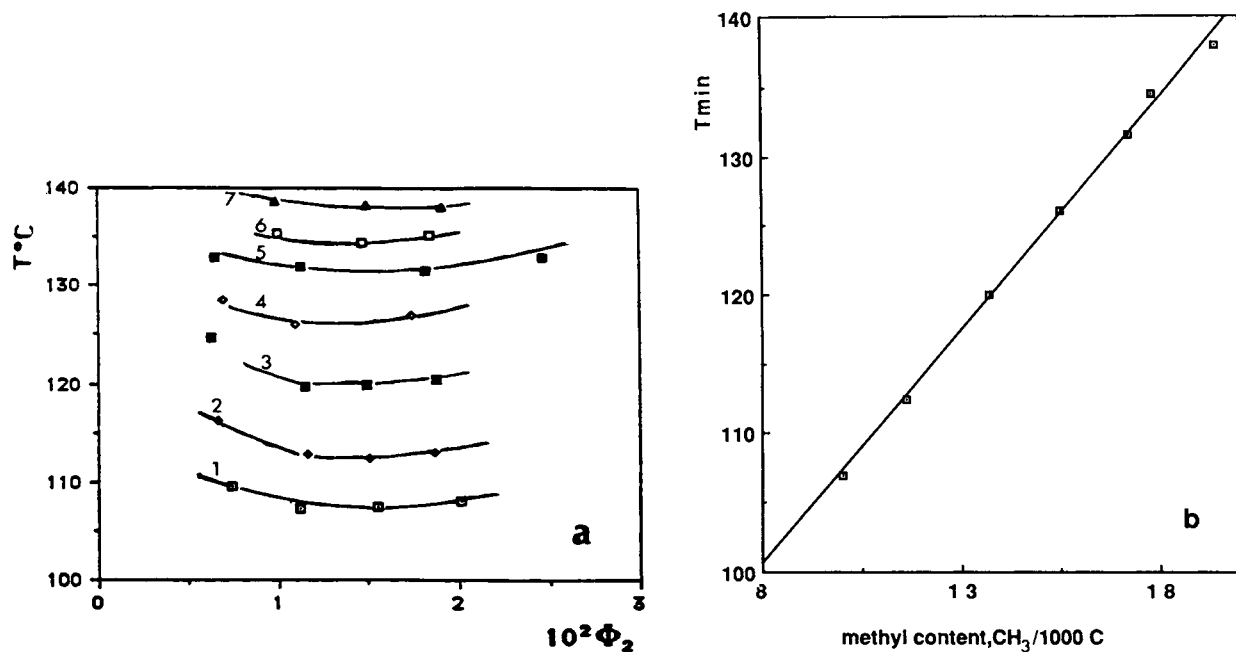
Figure 2   (a) Cloud-point curves $T_0(\phi_2)$ for the LCST fractions (1-7, Table I) in the n-pentane + n-hexane mixture for E(B). (b) T_{min} for LCST fractions in the n-pentane + n-hexane mixture vs. m for E(B).

lowed by a nonsizable turbidity peak at a narrow temperature interval. The rapid increase in turbidity occurs above 150°C (cf. Fig. 4). An evaluation of

the MW of a sample from the temperature of the first turbidity, T_0, has been reported in the literature and gives usually reasonable values [see the cloud-
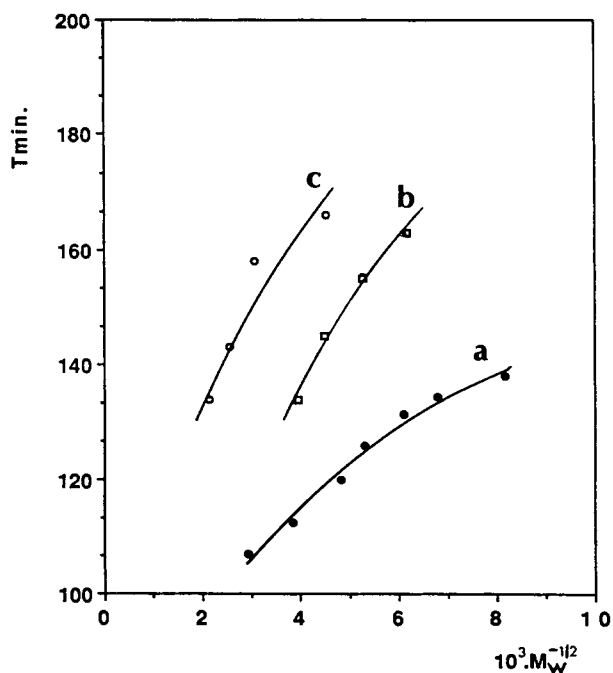
Figure 3 T_{min} vs. $M_w^{-1/2}$. Curve a: E(B), LCST fractions in n-pentane + n-hexane. Curve b: E(B), TREF fractions in 2,4-dimethylpentane. Curve c: E(O), TREF fractions in the same solvent.
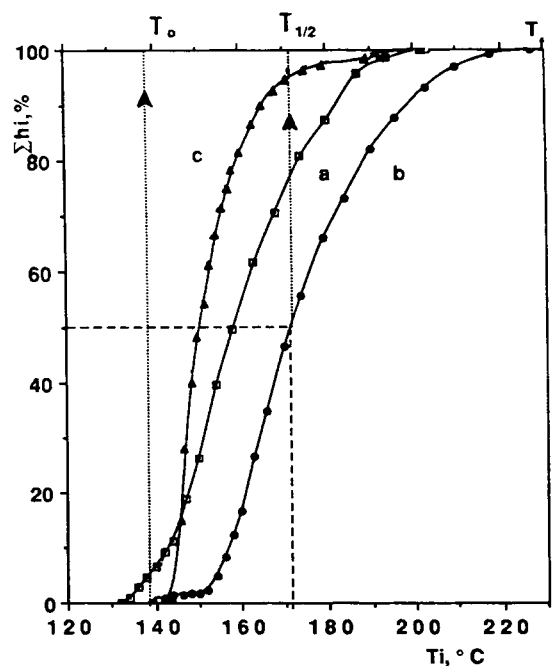
Figure 4   Examples of cumulative curves for unfractionated samples and one fraction. Curves a and b are for unfractionated E(O) and E(B). Curve c is LCST2. The characteristic temperatures have been marked on curve b.

point curves of Fig. 2(a)]. However, if the sample has a high MW trail as is the case of nonfractionated E(B), the information given by T_0 may be misleading. In Figure 4, the normalized cumulative turbidity peaks (Σh_1^*) of the E(B) and E(O) unfractionated samples (curves a and b) have been plotted against T_i. The range of temperature of the turbidity peaks is related to the sample polydispersity. The value read on the turbidity curve of 172°C for $T_{1/2}$ means that, for E(B), at about 30 K above the temperature of the first turbidity only half of the total turbidity has been evolved. For the fractions, the differences between T_f and $T_{1/2}$ and $T_{1/2}$ and T_0 are reduced, as seen in Table II and in Figure 4, where curve c corresponds to LCST2.

Molecular Weight and Polydispersity

In Table II, the characteristics of E(B) and E(O) and their fractions obtained from the thermograms are given. Columns 7-10 are calculated through the linear equation [eq. (4)], columns 11-14, with the equation of state [eq. (2)]. The averages are obtained using eqs. (5) for all the samples. The two calibrations are compared in Figures 5 and 6. The values of $T_\infty(m)$ needed to recover the SEC data for M_w have been plotted against m for the E(B) (x, ●) and E(O) (▲) TREF fractions in Figure 5. Both curves extrapolate for $m = 0$ to T_∞ found for
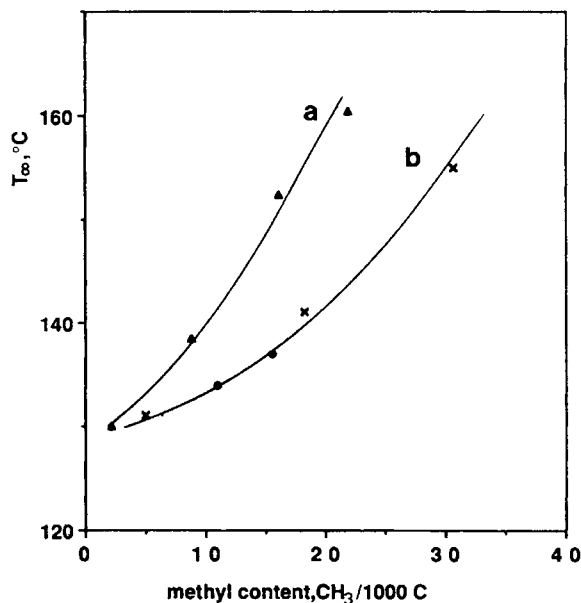

Figure 5 Characterization according to eq. (4): T. vs. m to fit M_w: curve a, E(O); curve b, E(B). For curve b: (x) TREF fractions; (●) LCST fractions.
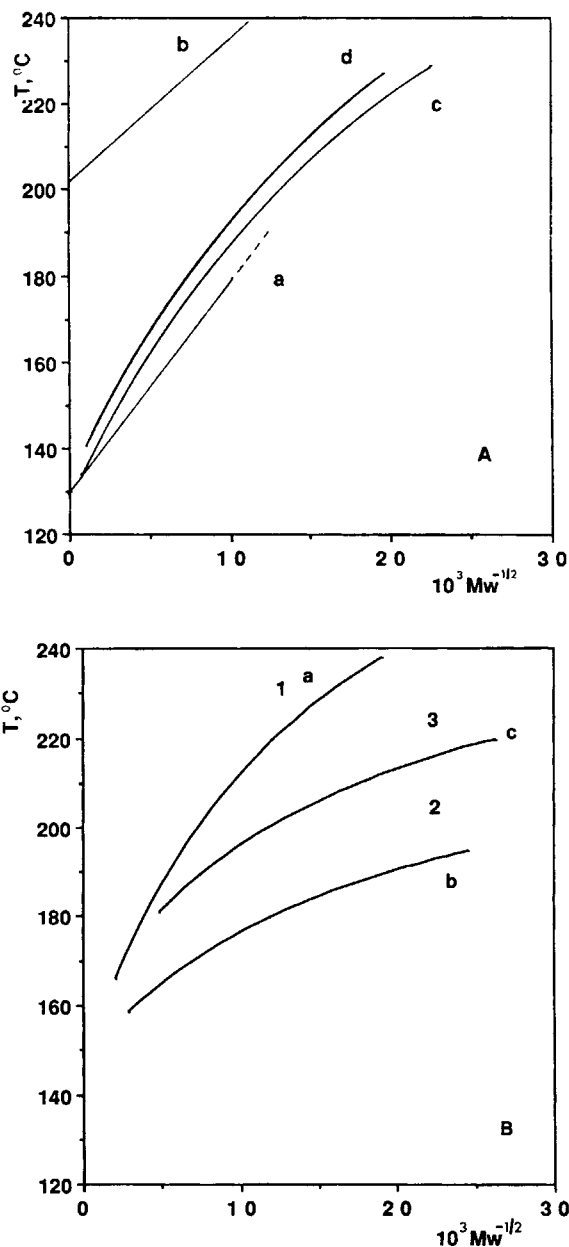

Figure 6 Calibration according to eq. 2. (A) $T(M_w^{-1/2})$ for two homogeneous and two heterogeneous polymers: (a) HDPE, (b) PP. (c) and (d) are for unfractionated E(B) and E(O), respectively. (B) $T(M_w^{-1/2})$ for fractions: (a) TREF1 for E(B); (b) TREF2 of E(O); (c) TREF3 of E(B).

the high-density PE. The bulky octyl comonomer is more efficient in lowering the PE density and increasing its LCST than is the butyl comonomer. In eq. (3), a constant value of B(= 4300) has been used, which has, in consequence, to lead to inaccurate polydispersity values but satisfactory results for

M_w of the different samples. In the abscissa of Figure 5, $M_w^{-1/2}$ could have been used instead of m since both are correlated. In Figure 6(A) and (B), which gives the results for the equation of state calculations, the $T(M^{-1/2})$ curves that lead from eq. (2) to the data of Table II are drawn. The four curves of Figure 6(A) correspond to two homogeneous polymers, namely, linear PE (a) and PP (b) and to two unfractionated heterogeneous samples E(O) (c) and E(B) (d), and the three curves of Figure 6(B), to three fractions TREF1 of E(B) (a), TREF2 of E(O) (b), and TREF3 of E(B) (c). The equation of state is seen to give values of M_w and M_w/M_n, in agreement with the SEC data for all the samples. For heterogeneous polymers, a linear relationship between T and $M^{-1/2}$ is not recommended.

Figure 7 is the cumulative curve of TREF3 in the ln-normal representation. M_w calculated point by point is equal to 110.2×10^3 whereas eqs. (6) lead to $139 \cdot 10^3$. This difference is due to the slight departure from linearity of the cumulative curve at high and low MW.

CONCLUSION

The comparison of TREF and LCST fractions has shown the specificity of the two methods. Characterization of the fractions by SEC has given the necessary information to choose the adequate parameters for the calibration of the LCST method, i.e., to relate the temperatures on the thermogram to molecular weights for a given value of m. The reproducibility of the LCST method, its simplicity, and its low cost are assets for its use to characterize the homogeneous and even heterogeneous polymers. For the latter, the range of chemical composition has to be known by another method such as IR analysis.

Figure 7 Cumulative curve in the ln-normal representation of TREF3 showing on almost linear correlation, characteristic of a normal distribution. M_w/M_n calculated from the slope is 3.8 with $n = 1$.

REFERENCES

1. S. D. Clas, D. C. McFaddin, K. E. Russel, M. V. Scammel-Ballock, and I. R. Peat, *J. Polym. Sci. Part A Polym. Chem.*, **25**, 3105 (1987).
2. D. C. McFaddin, K. E. Russel, and E. C. Kelusky, *Polym. Commun.*, **27**, 204 (1986).
3. B. K. Huter, K. E. Russel, M. V. Scammell, and S. L. Thompson, *Sci. Polym. Chem. Ed.*, **22**, 1383 (1984).
4. K. Shirayama, S. Kita, and H. Watabe, *Macromol. Chem.*, **151**, 97 (1972).
5. F. M. Mirabella and J. F. Johnson, *J. Macromol. Sci. Rev. Macromol. Chem.*, **C12**, 81 (1975).
6. L. Wild, T. R. Ryle, D. C. Knobeloch, and I. R. Peat, *J. Polym. Phys. Ed.*, **20**, 441 (1982).
7. (a) V. B. F. Mathot, H. M. Schoffeleers, A. M. G. Brands, and M. F. J. Pijpers, *Morphol. Polym. Proc. Europhys. Conf. Macromol. Phys.*, **17**, 363 (1986). (b) V. B. F. Mathot, *Pap. Proc. Polycon. LLDPE*, **1** (1984).
8. C. France, P. J. Hendra, W. F. Maddams, and H. A. Willis, *Polymer*, **28**, 710 (1987).
9. B. Schlund and L. A. Utracki, *Polym. Eng. Sci.*, **27**, 359 (1987).
10. S. C. Mathur and W. L. Mattice, *Macromolecules*, **20**, 2165 (1987).
11. R. Alamo, R. Domszy, and L. Mandelkern, *J. Phys. Chem.*, **88**, 6587 (1984).
12. D. E. Alxelson, *J. Polym. Sci. Polym. Phys. Ed.*, **20**, 1427 (1982).
13. A. Barbalata, T. Bohossian, K. Prochazka, and G. Delmas, *Macromolecules*, **21**, 286 (1988).

14. M. Besombes, J. F. Mengual, and G. Delmas, *J. Polym. Sci. Phys. Ed.*, **26**, 1881 (1988).

15. T. Bohossian, G. Charlet, and G. Delmas, *Polymer*, **30**, 1695 (1989).

16. P. I. Freeman and J. S. Rowinson, *Polymer*, **1**, 20 (1960).

17. I. Prigogine, A. Bellemans, and V. Mathot, *The Molecular Theory of Solutions*, North-Holland, Amsterdam, 1957.

18. G. Delmas, T. Somcynski, and D. Patterson, *J. Polym. Sci.*, **57**, 79 (1962).

19. R. A. Orwoll and P. J. Flory, *J. Am. Chem. Soc.*, **89**, 6822 (1967).

20. K. S. Siow, G. Delmas, and D. Patterson, *Macromolecules*, **5**, 29 (1972).

21. G. Delmas and P. de Saint-Romain, *Eur. Polym. J.*, **10**, 1133 (1974).

22. J. M. G. Cowie and I. J. McEwen, *Polymer*, **16**, 244, 933 (1975).

23. G. Charlet and G. Delmas, *Polymer*, **22**, 1181 (1981).

24. T. Bohossian, H. Benoit, and G. Delmas, to appear.

25. L. H. Peebles, *Molecular Weight Distribution in Polymers*, Wiley-Interscience, New York, 1971.